International Environmental Modelling and Software Society (iEMSs)
7th Intl. Congress on Env. Modelling and Software, San Diego, CA, USA,
Daniel P. Ames, Nigel W.T. Quinn and Andrea E. Rizzoli (Eds.)
http://www.iemss.org/society/index.php/iemss-2014-proceedings

Modeling Potential Environmental Impacts of Deep Aquifer CO2 Sequestration

Nigel W.T. Quinn PhD, P.E., D.WRE

Research Group Leader, HydroEcological Engineering Advanced Decision Support, Berkeley National Laboratory, 1 Cyclotron Road,
Berkeley, CA 9472, nwquinn@lbl.gov

Abstract: A promising measure for mitigating climate change is to store large volumes of CO_2 captured from large point-source carbon emitters in deep saline aquifers. In vulnerable systems, water resources impacts of large-scale CO_2 storage need to be evaluated and assessed before industrial-size storage projects get under way. In California's southern San Joaquin Basin the land surface uplift caused by large CO_2 injection projects land deformation could have the potential to create reverse flow along certain canal reaches, or to reduce canal deliveries to agricultural land and managed wetlands. The impact of CO_2 storage on shallow water resources was compared to the expected stresses on the groundwater and surface water systems from ongoing pumping using a version of the Central Valley Hydrological Model CVHM extended vertically to capture reservoir geology. Results of simulations demonstrated that such pumping-related deformations in the area might be one order of magnitude larger than those from CO_2 injection. In the basin the low permeability geological layers between shallow effectively limit pressure changes from migrating far in vertical directions, downward or upward.

Keywords: CO_2 sequestration; groundwater modeling; environmental impacts; land subsidence.

1. BACKGROUND

In California, the thick sediments of the Central Valley have been identified as prime targets for future geological carbon sequestration (GCS). The San Joaquin Basin has multiple saline aquifers and oil and gas reservoirs, which guarantee a large injection volume. Widespread shale seals found in the basins can serve as structural trapping, ensuring the natural long-term confinement of injected CO_2. In addition, there have been significant geological data collected from oil and gas operations, which facilitate reliable environmental assessments. Regionally, California's Central Valley has the largest CO_2 storage resource potential, in the range of 2.0 billion–4.1 billion metric tons. The southern portion of the Basin, the focus of our modeling study, is home to some of California's largest natural gas fields.

California's Central Valley is currently the home to over six million people, and generates over $20 billion in agricultural crops each year. The agricultural and urban development in the area depends on an intricate surface water distribution system that routes water from surrounding watersheds to the Central Valley, and on the presence of extensive aquifers that provide substantial amounts of irrigation water supply. Water resources impacts of large-scale CO_2 storage need to be evaluated and assessed before industrial-size storage projects get under way (Birkholzer et al., 2008, 2009; Zhao et al., 2011). Storing additional fluids in deep saline aquifers causes pressure changes and displacement of native brines, affecting subsurface volumes that can be significantly larger than the CO_2 plume itself. Environmental impacts on groundwater resources may result if the deep parts of the basin communicate effectively with shallower units. The deep sediments overlying the crystalline bedrock would be the main target of future CO_2 storage in the area. These sediments deposited in a marine environment form a succession of thick, porous and permeable, mostly saline aquifers separated by laterally persistent aquitards represented by marine shales (Birkholzer et al., 2008, 2009).

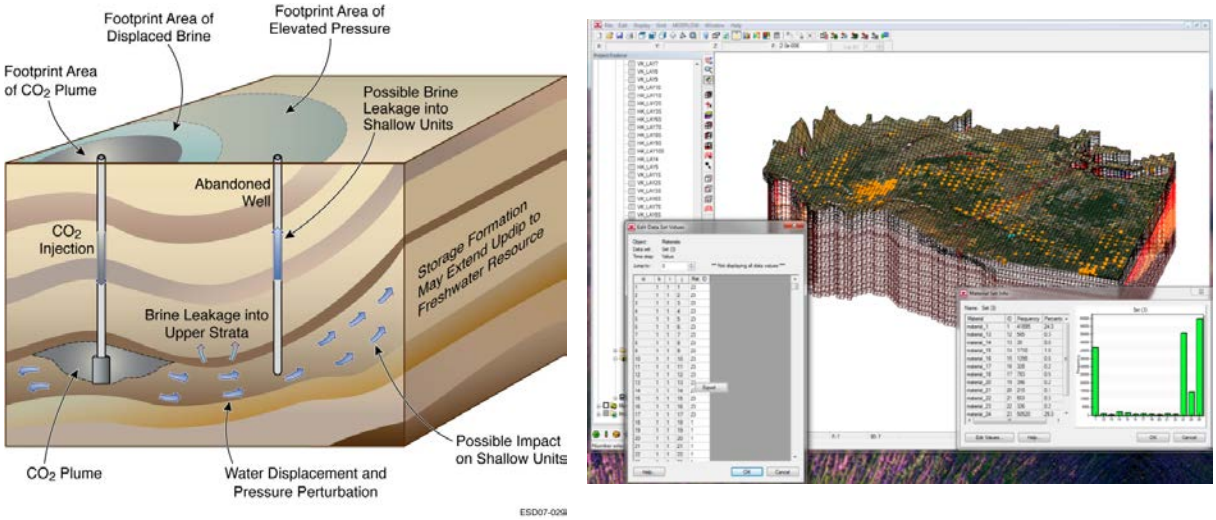

Figure 1. (a) Schematic showing different regions of influence related to CO_2 storage (Birkholzer et al., 2008, 2009; Zhou et al, 2011). (b) CVHM-Kern-FMP3 model domain and extended vertical mesh using Aquaveo GMS software (Quinn et al., 2013).

2. MODELING APPROACH

The three southern-most subareas from the Central Valley Hydrologic Model (CVHM - Faunt et al., 2009) was used to define the boundaries of the model study area (CVHM-Kern). The new model, (consistent with CVHM) has ten layers – the dominant aquitard - the Corcoran Clay Member of the Tulare Formation – was represented by layers four and five. The top layer was set equal to 50 ft (13 m) below land surface - the remaining layers ranged in thickness from 50 ft (13 m) to 400 ft (102 m) increasing by 50 ft (13 m) with each progressively deeper layer. The topographic surface is based on a 10 m lateral resolution DEM, which was converted to a 2D grid within Earthvision. Stratigraphic tops for all of the major stratigraphic units were digitized. These data were converted to elevation and 2D grids were generated for the top of each mappable unit. CVHM was originally developed using MODFLOW 2000 (MF2K) combined with the Farm Process (FMP) pre-processor (Schmid and Hanson, 2009). The code used in this project was a beta version of FMP3 with MODFLOW 2005 (Hanson, 2013). For the current application, the Friant-Kern Canal, the Cross-Valley Canal, and the Kern River are the only surface water conveyance facilities of consequence.

Six major types of data were provided in the CVHM-Kern-FMP3 model application. These include (1) hydrologic data such as precipitation (PRISM), well water levels, and streamflow; (2) land-use data including crop type; (3) surface-water deliveries and diversions; (4) water-use data from previous studies; (5) borehole lithologic data including texture information; and (6) subsidence and compaction data from extensometers (Faunt et al., 2009). A texture model was used to estimate hydraulic conductivity for every cell in the published CVHM-FMP3 model based on a methodology developed earlier work by Laudon and Belitz (1991). The textural analysis was based on the percentage of coarse-grained texture, compiled from driller's logs of wells and boreholes. The FMP3 beta module dynamically allocates groundwater recharge and groundwater pumpage on the basis of crop water demand, surface-water deliveries, and depth to the water table (Schmid and Hanson, 2009; Hanson, 2013 personal communication). In FMP3 the farm irrigation diversion requirement is calculated from consumptive use, effective precipitation, groundwater uptake by plants, and on-farm efficiency. The Streamflow Routing Package (SFR1) was linked to facilitate the simulated conveyance of surface-water deliveries (Schmid and Hanson, 2009). If surface-water deliveries do not meet farm delivery requirements then groundwater pumping is invoked to meet irrigation demand.

Twenty-one additional layers were inserted between the bottom of the existing CVHM-Kern-FMP3 model and the basement rock layer that defines to bottom boundary. In plan-view, the grid structure of the deeper geologic model layers was made identical to the existing 10-layer model. The lowest layers of the geologic model below the injection zones were sloped to conform to the basement geologic boundary. Model layering above the zone of pumping was represented by layers of uniform

thickness. Refined layering was created in the vicinity of the CO_2 injection wells in the Vedder Sand and Stevens Sand geological formations was made to improve simulation accuracy. Based on the geological model assignment, the model properties of the deeper layers were then made consistent with a previous Deep Basin Reservoir Simulation Model developed using the Berkeley National Laboratory TOUGH2 code (Zhang and Pruess, 2008; Zhao et al., 2011).

2.1 Model scenario formulation

Two CO_2 injection scenarios were simulated - the first with injection into the Vedder Sand formation only; the second with injection into both the Vedder and Stevens Sand formation. This second scenario was developed (1) to evaluate the cumulative impact of multiple injections in the same region and (2) to analyze for possible project interference. Both of these scenarios were compared to a base simulation in which the same level of groundwater extraction continues in the upper formations (upper 10 layers simulated by the CVHM-Kern-FMP3 model), but there is no CO_2 injection. Injection rates were set equivalent to 5 million tons of CO_2 at the Vedder Sand and Stevens Sand formation locations - this is roughly equivalent to half the CO_2 at a 90% capture rate from local CO_2 generating sources - sources that emitted more than 200,000 tons during the most recently available inventory year. Using the same injection rate for both injection simulations allowed a direct comparison of effects, particularly any cumulative effects, from adding a second injection not far away in a different geologic unit. Volumetric CO_2 injection rates were set equivalent to 7,200,000 m^3/yr per injection project. The MODFLOW 2005 code does not simulate multi-phase flow (unlike the TOUGH2 simulation code – Zhang et al, 2008) – hence an assumption was made that the injected volume of supercritical or dense-phase CO_2 displaces an equivalent volume of fluid in the formation (Quinn et al., 2013). The CO_2 equivalent is injected at a constant rate for the duration of the simulation. This typically results in near-field pressures that can increase significantly over time if the formation is confined. Pressure leakage from the formation can occur if the caprock is discontinuous, or when internal pressure is sufficient for the injected CO_2 to find a flow path into a more permeable formation.

2.2 Model observation locations

When running CVHM-FMP3 the response was recorded not only at the injection site (i.e., in the grid cell where injection takes place), but also at strategically located observation points, to provide a window on how the fluid pressure changes in different parts of the same geologic formation or in adjacent formations. Two observation locations were chosen for each CO_2 injection well: (a) a hydrologic monitoring location “Vedder hydro,” about 6 km updip of the Vedder formation injection location to the east; (b) a location “Vedder geo” updip of that point to the east, where the Vedder formation is in contact with the base of the shallow mesh (about 23 km east of the injection location); (c) a hydrologic monitoring location “Stevens hydro” about 5 km west of the Stevens formation injection location; and (d) a location “Stevens geo” about 6 km northeast of the Stevens formation injection well, where the Stevens formation overlies a portion of the Vedder formation. If the pressure response from both injection wells reached this fourth location - we expected to observe a small additive effect on head change and uplift. (Note: a change in pressure of 1 MPa converts to a hydraulic head change of about 100 m.)

3. SIMULATION RESULTS

3.1 Vertical profiles of head and displacement response

Vertical profiles of head distribution at years 0.1, 10, 25, and 50 during CO_2 injection into the Vedder and Stevens formations. The profiles are shown at the injection location in the Vedder formation; injection occurs into Layers 26 and 27. The strong head-buildup response to the injection is clearly centered initially within the injection formation. With time, the head buildup increases in amplitude, dominated by injection into the Vedder layers. However, the profile appears to become bi-modal by year 10, suggesting perhaps some small influence from the injection at the shallower Stevens

location. As expected, the profile reaches its maximum amplitude by year 50, the time when CO_2 injection stops.

In the shallow formations—notably the layers affected by groundwater pumping—dewatering of these zones at current rates of extraction appears to lead to a significant loss in groundwater head, which will lead to continued land subsidence as pressure heads are further reduced below the pre-consolidation heads associated with the onset of inelastic deformation. This, of course, is a water-resources impact due to pumping mostly for agricultural purposes, and has nothing to do with deeper CO_2 injection.

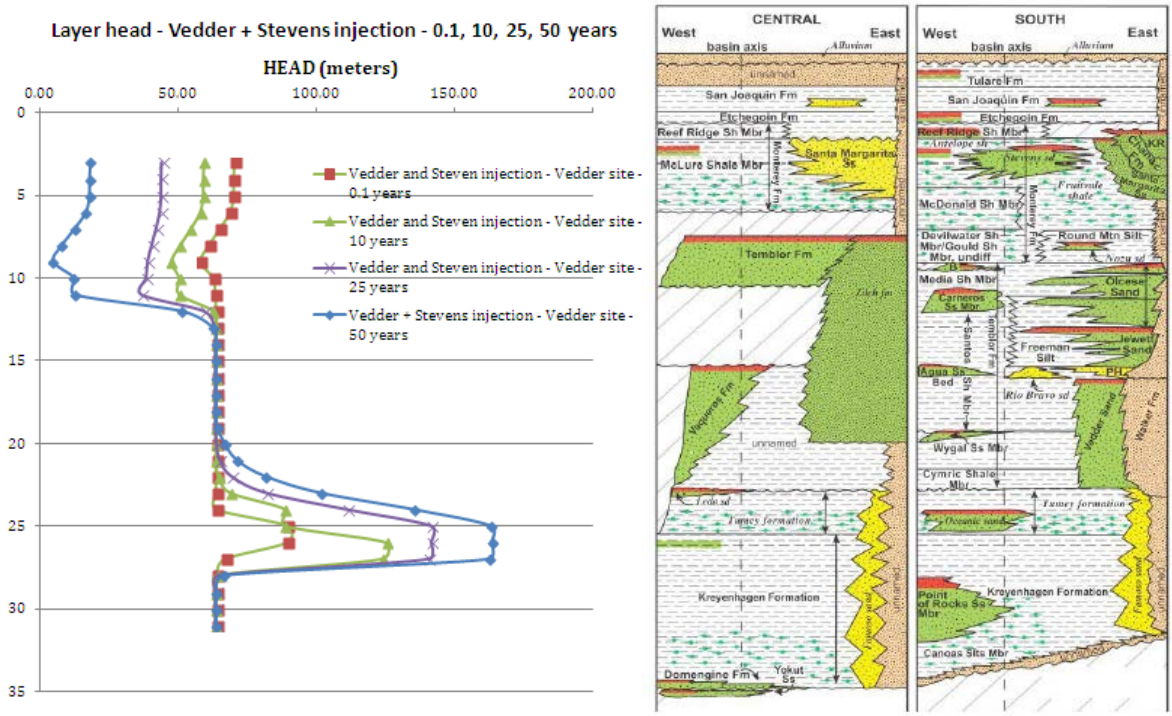

Figure 2. (a) Head profiles for the injection simulation into the Vedder and Stevens sand formations observed at the Vedder site for 0.1, 10, 25 and 50 years. Depth in the vertical axis is represented as "layer number." There are 31 vertical layers. (b) Generalized stratigraphic section for the CVHM-Kern model region showing location of Vedder and Stevens sand formations (Quinn et al., 2013).

In both injection and pumping instances, as the head response increases in amplitude it also migrates upward and downward into adjacent layers. This is a slow process, however, due to the low permeability of intervening shale formations, and the overall propagation distance is not very large. In the deeper layers, injection is felt in an upward direction up to about Layer 20 at the end of 50 years but only migrates downward to Layer 28 in the same time interval. In the shallow layers, the Corcoran Clay appears to prevent the pressure response to pumping from moving much higher than Layer 5 and much lower than Layer 12.

The vertical profiles from the CVHM-Kern-FMP3 model were checked for consistency with the same injection scenario modeled using the Deep Basin Reservoir Simulation Model. That the head increase in Figure 2 was less than the TOUGH2 base case is to be expected, since (a) the TOUGH2 numerical grid is much more refined near the injection wells, (b) the partially compartmentalized nature of the Vedder formation is better represented in the TOUGH2 numerical grid which explicitly accounts for major faults, and (c) the TOUGH2 simulations account for buoyancy pressure of free-phase CO_2. There consistency between the two models with regards to the strong effect of over- and underlying shale units on retarding the vertical pressure propagation is similar in both simulation results. The simulation results from the CVHM-Kern-FMP3 model provide a sufficiently accurate representation of pressure perturbation in the deep formations. In the transition zone directly into the deeper layers near the injection into the Vedder formation (Layers 25, 26 and 27), the head and displacement responses completely change, from a system influenced by shallow pumping of groundwater to a

system influenced by deep CO_2 injection. Layer 21 is above the injection horizon and Layer 26 is one of the injection layers. For both injection scenarios, the head in Layer 26 rises strongly (as expected) to around 160 meters by the end of the 50-year injection period. The increase follows a roughly linear increasing trend after the reservoir volume is pressurized initially. Displacement in Layer 26 represents a modest uplift of about 5 to 6 cm at 50 years. In Layer 21, above the injection horizon, we observe a modest head increase, which represents the influence of deeper injection retarded by the low permeability of the intervening shale layers. The uplift in Layer 21 is larger, though, than in Layer 26. This reflects the fact that the uplift within a vertical column is roughly the cumulative effect of pore expansion in different model layers. The uplift in Layer 21 is roughly equal to the uplift within the injection layer (Layer 26), plus the vertical expansion caused by head increases in Layers 25, 24, 23, and 22. The baseline results in both deep layers (Layers 21 and 26) show essentially zero changes over time. In other words, the shallow groundwater pumping causes no measurable response in the deeper layers, another sign that there is no hydraulic communication between them. The two injection scenarios show identical response at the Vedder injection location. In other words, the additional injection occurring in the Stevens formation, about 17 km away and separated stratigraphically, does not affect the head and displacement conditions at the Vedder injection location.

The observation results at the locations associated with the Stevens formation injection site show the same general trends as the Vedder observation wells. Heads in the shallow formation model exhibit a general downward trend as the groundwater aquifer continues to be dewatered and the overlying agricultural land subsides in response. What is more pronounced than in the Vedder locations is the stronger uplift signal seen in the simulation case with CO_2 injection into both formations, with clear deviation of this case from the other simulation cases. This suggests that the injection into the Stevens generates a head and uplift response that is slightly larger than that in the Vedder, which is an expected result because of the smaller formation extent and the more pronounced compartmentalization.

The CO_2 injection into the Stevens *and* the Vedder formations, results in a much stronger head and displacement response than in the other scenarios. At both locations, injection into the Stevens formation creates head changes of up to 150 m and displacement of up to16 cm. The smaller spatial extent of the Stevens formations causes the head and displacement perturbations to be stronger than in the Vedder, though the injection volumes are the same. The baseline results and those from Scenario 1, the Vedder-only injection, are identical for the Stevens “hydro” location, meaning that CO_2 injection into the Vedder has no effect there. This location is about 4 km west of the Stevens injection, away from the influence of the Vedder unit, which is farther east. In contrast, at the Stevens “geo” location, the Vedder-only injection causes uplift of about 4 cm in the Stevens, compared to zero uplift in the baseline simulations and about 16 cm uplift from the combined Vedder and Stevens injections. At this location, the Stevens formation overlies a portion of the Vedder formation and the observed uplift is the cumulative result from both injections.

3.2 Contour plots of head at 0.1, 10, 25 and 50 years

The spatial extent of head changes due to pumping in shallow units and CO_2 injection in deep reservoirs is shown below in contour plots for selected horizontal model layers. Head changes in Layer 6 for the baseline scenario at 0.1, 10, 25, and 50 years are virtually identical with those for two CO_2 injection scenarios. Shallow-formation aquifer dewatering from continued groundwater pumping shows up in mostly the center of the model as a reduction in hydraulic head, becoming very pronounced by 50 years. Layer 10, near the interface between the shallow model and the deeper vertical extension, shows a similar but slightly less pronounced behavior in terms of significant decline in hydraulic head due to groundwater pumping.

A very different picture of head changes can be observed in the deeper formations for head changes in the baseline scenario, the Vedder-formation-only injection, and the combined Vedder and Stevens formation injection, respectively). Results for Layer 21 of the model grid are shown in Figure 3, which comprises a substantial fraction of the Stevens formation in the west and intersects the updipping Vedder formation further east. The baseline scenario shows no considerable changes in hydraulic heads in this layer during the 50-year simulation period. This confirms again that shallow groundwater pumping has no effect on the deep hydrologic systems. In contrast CO_2 storage in the Vedder

formation causes considerable and extensive head increases as indicated an elongated north-south trending zone where Layer 21 intersects the Vedder formation, the hydraulic head perturbation in the Vedder extends several tens of kilometers away from the injection location. The added effect of injecting into both the Vedder and Stevens formations (Figure 3) shows a distinct area of head increase in the southwest portion of the model domain, where Layer 21 coincides with the Stevens formation. As observed before, the head changes in the Stevens are stronger than in the Vedder, because the same volume of CO_2 is injected into a smaller, more compartmentalized geologic unit.

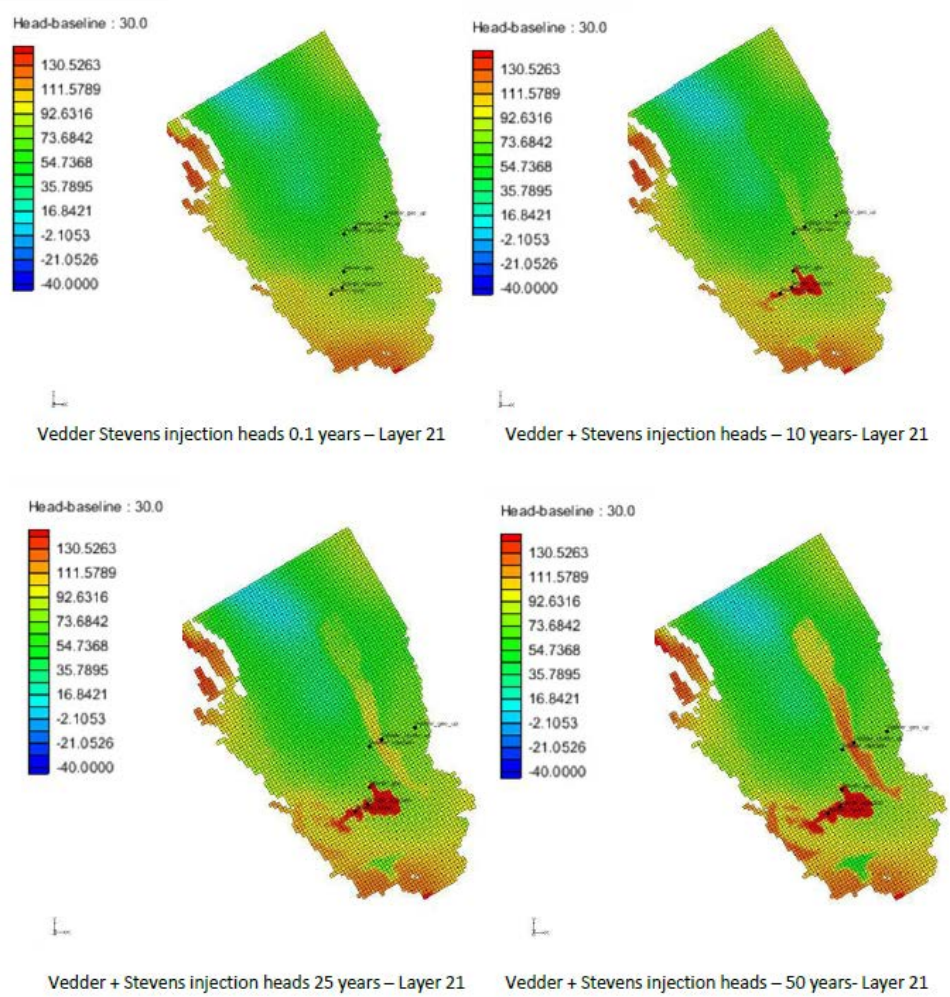

Figure 3. Vedder and Stevens injection head contours (meters) for Layer 21 at 0.1 years, 10 years, 25 years, and 50 years. Plots show distinct head increases which are more pronounced in the shallow Stevens formation injection.

3.3 Contour plots of vertical displacement at 0.1, 10, 25 and 50 years

Figure 4. illustrates vertical displacement in Layer 6 for the baseline scenario at 10, 25, and 50 years. A large area within the model domain may experience significant subsidence, a result of the assumed continued pumping of groundwater without countermeasures. Subsidence is strongest after 50 years, with extended regions showing several meters of displacement. Compared to the meter-scale subsidence effects from groundwater pumping, the injection-induced upward displacement from deep storage of CO_2 is on the order of centimeters to perhaps decimeters.

Considering the displacement behavior in the deeper layers (Layer 21), the baseline displacements, while showing some simulation artifacts at the boundaries, are very small and mostly constant over the simulation period. Results for the Vedder only injection show a wide north-south trending region of vertical uplift (up to 10 cm). This is the region where the Vedder formation underlies or intersects

Layer 21 and where head increases are large enough to cause measurable uplift. Figure 5, which simulates the combined Vedder and Stevens injection shows an additional area of relatively strong uplift (up to 20 cm) in the south, reflecting the spatial extent of head increase in the Stevens formation. Again, the overall magnitude of uplift caused by deep injection is dwarfed by the meter-scale subsidence caused by pumping in the shallower units.

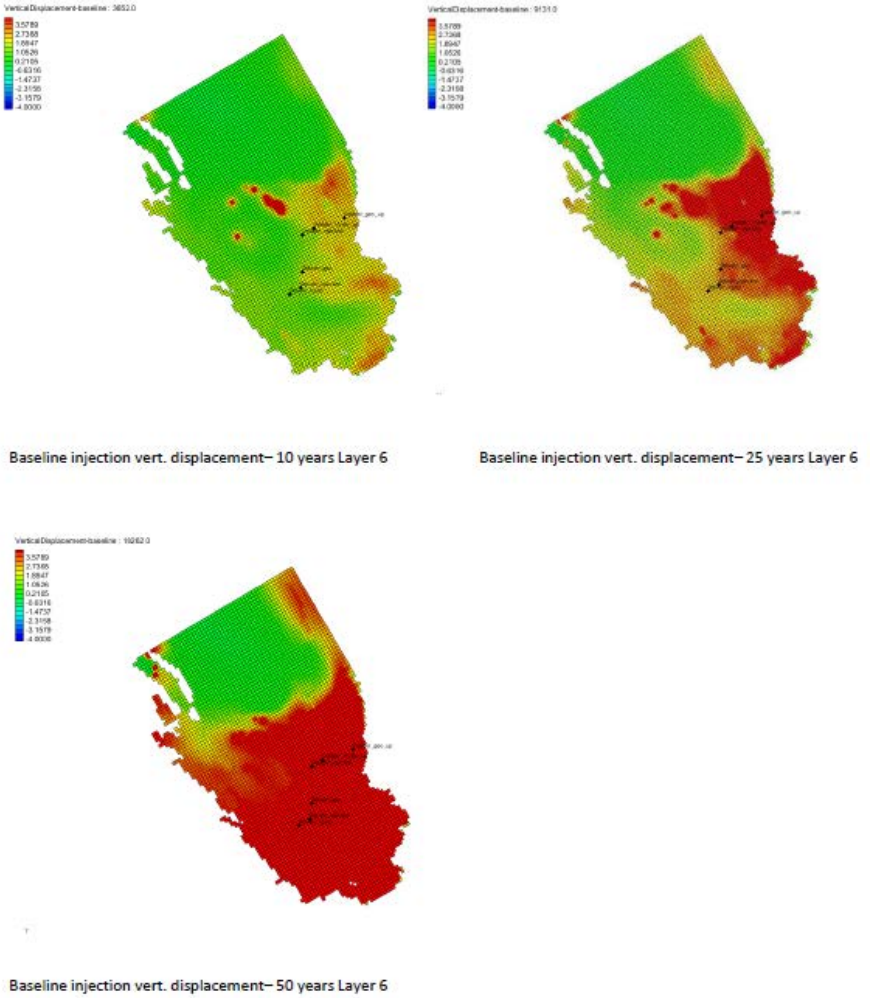

Figure 5. Baseline vertical displacement contours (meters) for Layer 6 at 10 years, 25 years, and 50 years. Positive values indicate subsidence, negative values indicate uplift.

4. SUMMARY AND DISCUSSION

The CVHM-Kern-FMP3 model was applied to three simulation scenarios, the first a baseline scenario with ongoing groundwater stress due to irrigation pumping - but no CO_2 injection. The CO_2 injection scenarios annually injected 5 million tons into the deep Vedder sand formation and combined Vedder and Stephens sand formations respectively. The induced head and vertical displacement perturbations were compared at several locations throughout the domain and at various depths ranging from shallow to deep. The following observations were made:

(a) While ongoing stresses from pumping in shallow aquifers have strong effects on the shallow groundwater regime and CO_2 injection causes strong perturbation in the deep subsurface, these effects are largely independent of each other, at least in the absence of localized flow paths (such as leaky faults or fractures). The many geological layers many of which are of very low permeability, limit pressure changes from migrating far in vertical directions, downward or upward.

(b) There is a potential for CO_2 injection to cause extensive land-surface uplift; for the scenarios simulated - the maximum vertical displacement caused by injection was about 20 cm. These

upward deformations need to be considered in the context of ongoing subsidence from groundwater pumping. Our simulations demonstrate that such pumping-related deformations in the area might be one order of magnitude larger than those from CO_2 injection.

(c) The two injection scenarios provided useful observations with respect to CO_2 sequestration in stacked reservoirs. Despite the Vedder and Stevens formations being in close proximity and having partial overlap there was little interaction in terms of pressure perturbations as a result of vertical separation by low-permeability units. With identical CO_2 injection rates and volumes - the Stevens formation exhibited stronger head buildup than the Vedder, a result of the higher degree of compartmentalization in the Stevens. Wherever the two formations overlapped vertically and exhibited head increases - the effect on overall vertical displacement was cumulative.

The simulation results suggest that large CO_2 storage projects should have minimal impact on shallow groundwater and surface water systems if, as in the scenarios considered in here, thick layers of shales and sands separate the deep CO_2 injection layers from shallow aquifers. The study did not, however, look into the potential for leakage of CO_2 and/or brine in localized pathways nor does it consider the possibility of pressure-induced fault activation, or "induced seismicity". This question could be addressed using the integrated shallow-to-deep models developed in this study.

6. ACKNOWLEDGMENTS

This paper summarizes work performed by a project team including Dr.Jens Birkholzer, Dr. Haruko Wainwright, Preston Jordan and Dr Quanlin Zhou of Berkeley National Laboratory under grant funding provided by the California Energy Commission. The project would not have been successfully completed without their help. The author also thanks Drs. Claudia Faunt and Randy Hanson, USGS for their help with the CVHM model code and permission to use a beta version of FMP3. Hoang Tran from Aquaveo Inc. provided excellent support on GMS.

7. REFERENCES

Birkholzer, J.T., Zhou, Q., Zhang, K., Jordan, P., Rutqvist, J., Tsang, C.-F. (2008). Research Project on CO_2 Geological Storage and Groundwater Resources: Large-Scale Hydrogeological Evaluation and Impact on Groundwater Systems, Annual Report October 1, 2007 to September 30, 2008, Lawrence Berkeley National Laboratory, Berkeley, CA.

Birkholzer, J.T., Zhou, Q. (2009). Basin-scale Hydrogeologic Impacts of CO_2 Storage: Capacity and Regulatory Implications, *Int. J. Greenh. Gas Con.,* 3(6), 745-756.

Faunt, C.C., Hanson, R.T., Belitz, K., Schmid, W., Predmore, S.P., Rewis, D.L., McPherson, K. (2009b). Numerical Model of the Hydrologic Landscape and Groundwater Flow in California's Central Valley, in "Groundwater Availability of the Central Valley Aquifer, California," edited by Faunt, C.C., U.S. Geological Survey Professional Paper 1766, 225 p.

Laudon, J., Belitz, K. (1991). Texture and Depositional History of Late Pleistocene–Holocene Alluvium in the Central Part of the Western San Joaquin Valley,

Quinn, N.W.T., H. Wainwright, P. Jordan, Q. Zhou, J.T. Birkholzer. 2013. Potential Impacts of Future Geological Storage of CO2 on the Groundwater Resources in California's Central Valley Simulations of Deep Basin Pressure Changes and Effect on Shallow Water Resources. Final Project Report to the California Energy Commission, Berkeley National Laboratory, Berkeley, CA.

Schmid, W., Hanson, R.T. (2009). The Farm Process Version 2 (FMP2) for MODFLOW-2005 – Modifications and Upgrades to FMP1. U.S. Geol. Survey Techniques and Methods 6–A32.

Zhang, K., Wu, Y.S., Pruess, K. (2008). User's Guide for TOUGH2-MP – A Massively Parallel Version of the TOUGH2 Code. Report LBNL-315E, Lawrence Berkeley National Laboratory, Berkeley, CA, USA.

Zhou, Q., Birkholzer, J.T., Wagoner, J.L. (2011). Modeling the Potential Impact of Geologic Carbon Sequestration in the Southern San Joaquin Basin, California, The Ninth Annual Carbon Capture & Sequestration Symposium, Pittsburgh, PA.